FORWARD AND BACKWARD CRITICAL SPEEDS AND FORCED RESPONSE OF AN OVERHUNG ROTOR WITH ASSYMETRICAL BEARING SUPPORTS

By

E. J. Gunter, Ph.D.
Director, Rotordynamics Laboratory

Department of Mechanical and Aerospace Engineering
University of Virginia
Charlottesville, VA 22903

December 1993

SCHOOL OF
ENGINEERING
& APPLIED SCIENCE

University of Virginia
Thornton Hall
Charlottesville, VA 22903

EQUATIONS OF MOTION OF AN OVERHUNG SHAFT INCLUDING DISC GYROSCOPIC EFFECTS

The following derivation is adopted from the original derivation of F.M. Dimentberg "Flexural Vibrations of Rotating Shafts," Butterworths 1961, pp. 61-67. The derivation is based upon the influence coefficient method. Figure 1 represents an overhung disk on a massless elastic shaft. The shaft is supported by simple bearings of infinite stiffness. The bearing span is L and the disk overhung distance is a.

If rotor acceleration is ignored, then the motion of the disk is described by 4 equations of motion. These equations relate the x, y translations of the disk and ϕ_x and ϕ_y which represent the angular displacements or rotations of the disk.

In the derivation of the equations of motion for the overhung disk, a right handed coordinate system will be used. This is the standard procedure used in finite element analysis in order for the stiffness matrix to be positive and symmetric. Therefore positive values of X and Y represent positive displacements respectively of the disk from the x and y axes, respectively. Likewise, positive rotations ϕ_x and ϕ_y represent small rotations of the disk about the x and y axes, respectively.

In this derivations of the overhung disk including gyroscopic moments, as adopted from Dimentberg, small displacements and rotations are assumed. This linearizes the equations of motion. If large displacements and rotations are assumed, then the Eulerian angles are normally used. These angles are expressed in a rotating coordinate system and represent the disk rotation, precession and nutation angles. The use of the standard Eulerian angles for rotor dynamics is undesirable as this leads to nonlinear equations of motion. If the assumption of small disk angles is assumed, then Dimentberg, Timoshenko, and Yamamoto have shown that the gyroscopic equations may be represented by linearized equations with the rotations expressed in an absolute reference frame.

The deflections and rotations at the overhung disc are expressed in terms of the forces and moments acting on the disc for the $x - z$ plane as shown in Figure 2.

$$X = \left(\frac{a^3}{3EI} + \frac{a^2 L}{3EI}\right) P_x + \left(\frac{a^2}{2EI} + \frac{aL}{3EI}\right) M_y \tag{1}$$

$$\phi_y = \left(\frac{a^2}{2EI} + \frac{aL}{3EI}\right) P_x + \left(\frac{a}{EI} + \frac{L}{3EI}\right) M_y \tag{2}$$

The deflection and slope y and ϕ_x of the shaft for the $y - z$ plane are given by

$$Y = \left(\frac{a^3}{3EI} + \frac{a^2 L}{3EI}\right) P_y - \left(\frac{a^2}{2EI} + \frac{aL}{3EI}\right) M_x \tag{3}$$

$$\phi_x = -\left(\frac{a^2}{2EI} + \frac{aL}{3EI}\right) P_x + \left(\frac{a}{EI} + \frac{L}{3EI}\right) M_x \tag{4}$$

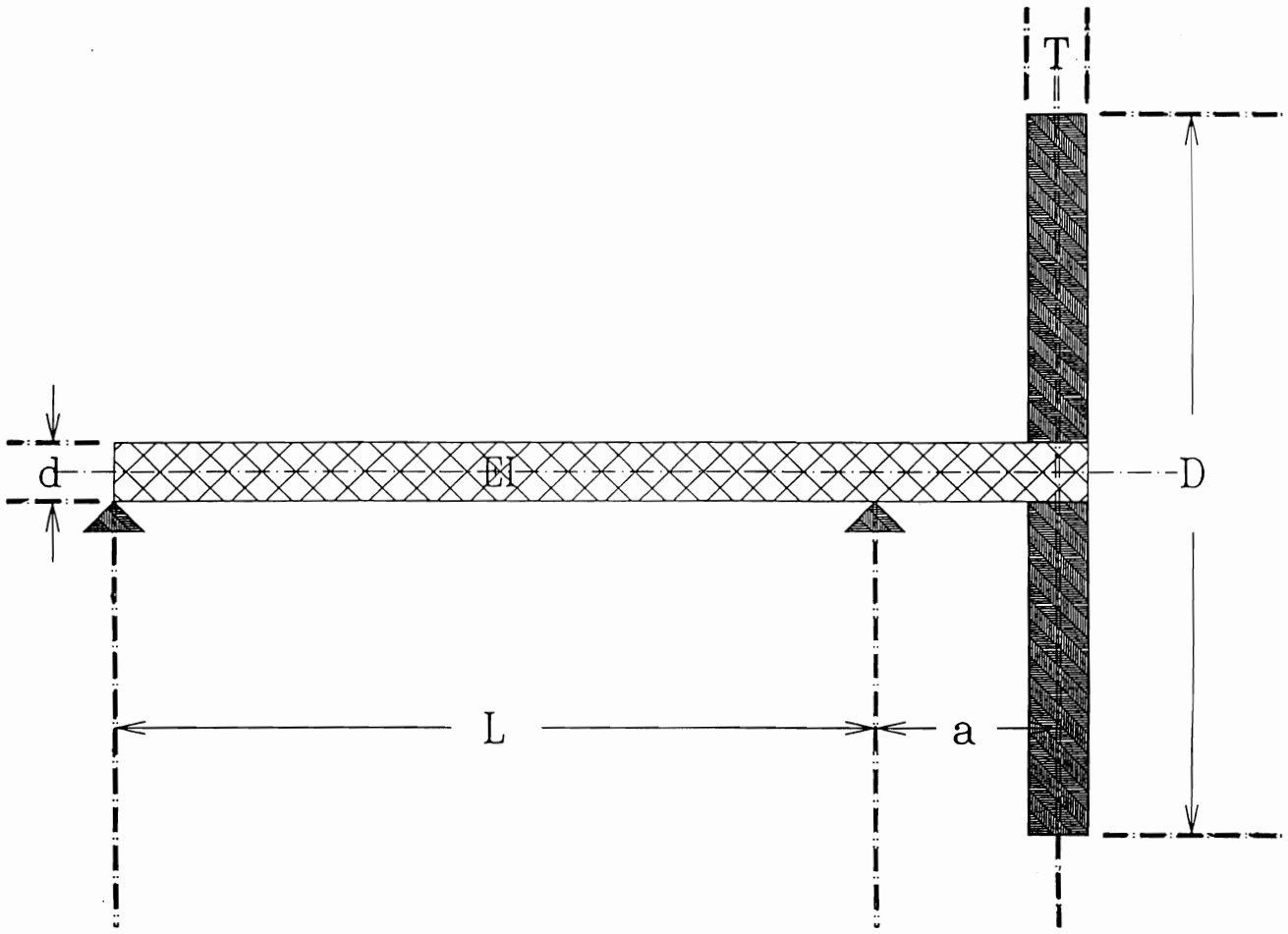

Fig. 1 Schematic of Overhung Rotor

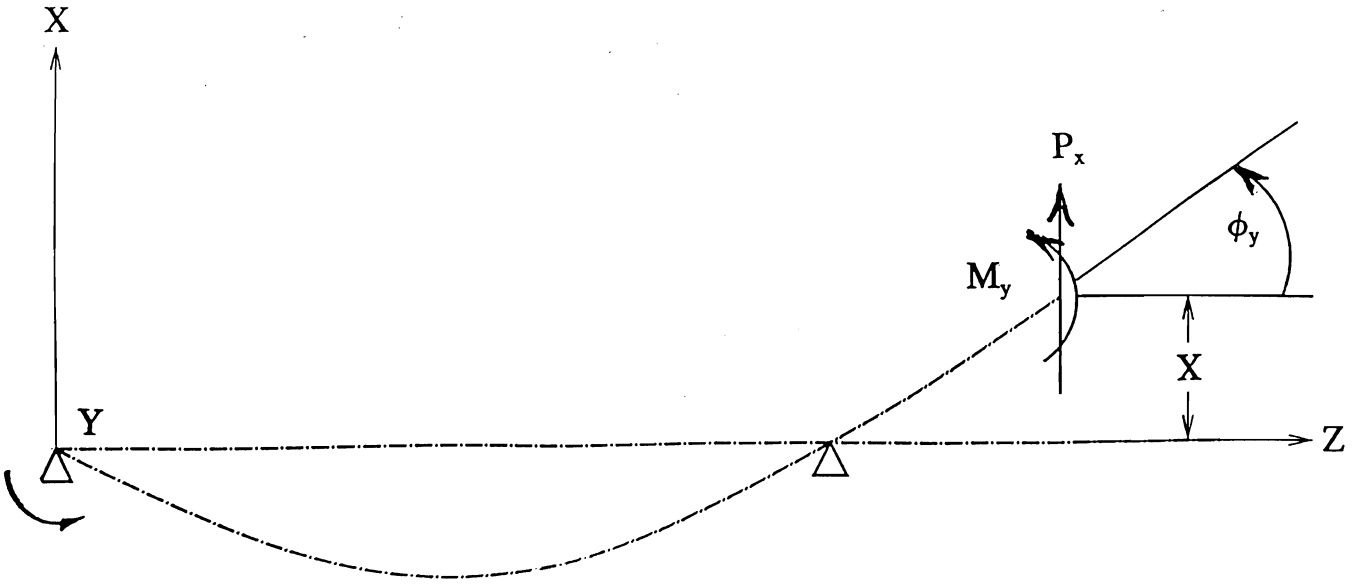

(a) X-Z plane of overhung shaft showing force and moment P_x and M_y

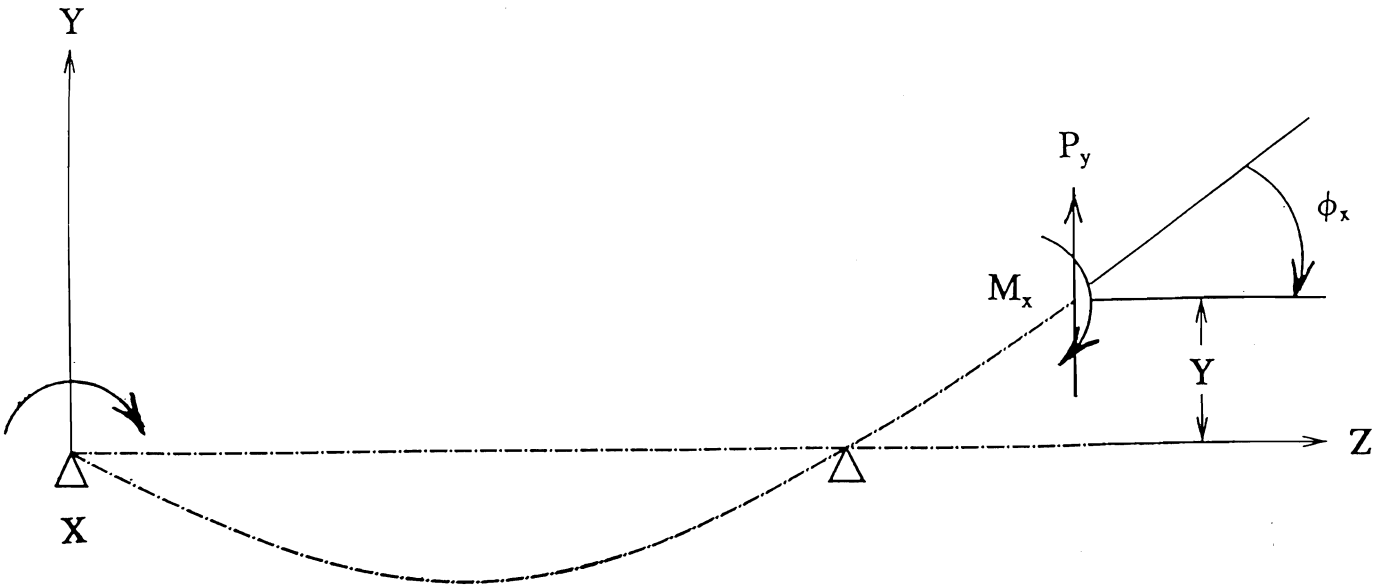

(b) Y-Z plane of overhung shaft showing force and moment P_y and M_x

Fig. 2 Overhung Shaft With Reaction Forces and Moments

The terms $P_{x,y}$ and $M_{x,y}$ represent the external forces and moments acting on the shaft at the disk overhang location. The right-hand rule is used for both the forces and bending moments acting at the end of the shaft.

The shaft deflections and rotations at the overhung disk location may be expressed in matrix form using the four influence coefficients a_{ij}.

The influence coefficients are defined as

$$a_{11} = \frac{a^3}{3EI} + \frac{a^2 L}{3EI} \quad ; \quad a_{12} = \frac{a^2}{2EI} + \frac{aL}{3EI}$$

$$a_{21} = \frac{a^2}{2EI} + \frac{aL}{3EI} \quad ; \quad a_{22} = \frac{a}{EI} + \frac{L}{3EI}$$

At this point the deflections of the shaft in the $x-z$ and $y-z$ planes are uncoupled from each other. The deflections and rotation in the $x-z$ plane may be expressed in terms of the influence coefficients as

$$\left.\begin{aligned} X &= a_{11}\, P_x + a_{12}\, M_y \\ \phi_y &= a_{21}\, P_x + a_{22}\, M_y \end{aligned}\right\} \tag{5}$$

In matrix form this would be expressed as

$$\left\{ \begin{array}{c} q_1 \\ \\ q_2 \end{array} \right\} = \left[\begin{array}{c} \\ \mathbf{a} \\ \\ \end{array} \right] \left\{ \begin{array}{c} F_1 \\ \\ F_2 \end{array} \right\} \tag{6}$$

Where

$$q_1 = X \quad ; \quad q_2 = \phi_y$$

$$F_1 = P_x \quad ; \quad F_2 = M_y$$

and for the $y-z$ plane

$$\left\{ \begin{array}{c} q_3 \\ \\ q_4 \end{array} \right\} = \left[\begin{array}{c} \\ \mathbf{a} \\ \\ \end{array} \right] \left\{ \begin{array}{c} F_3 \\ \\ F_4 \end{array} \right\} \tag{7}$$

Where

$$q_3 = Y \quad ; \quad q_4 = -\phi_x$$

$$F_3 = P_y \quad ; \quad F_4 = -M_x$$

The influence coefficient matrix [**a**] may be inverted to obtain the shaft stiffness matrix [**K**] such that

$$\left\{ \begin{array}{c} F_1 \\ \\ F_2 \end{array} \right\} = \left[\begin{array}{cc} K_{11} & K_{12} \\ \\ K_{12} & K_{22} \end{array} \right] \left\{ \begin{array}{c} q_1 \\ \\ q_2 \end{array} \right\} \tag{8}$$

The stiffness coefficients K_{ij} for the overhung shaft are as follows:

$$K_{11} = \frac{12EI}{a^3}\left(\frac{3a+L}{3a+4L}\right) \quad ; \quad K_{12} = -\frac{6EI}{a^2}\left(\frac{3a+2L}{3a+4L}\right)$$

$$K_{21} = -\frac{6EI}{a^2}\left(\frac{3a+2L}{3a+4L}\right) \quad ; \quad K_{22} = \frac{4EI}{a}\left(\frac{3a+3L}{3a+4L}\right)$$

Solving the system equations with respect to P_x and M_y, the following is obtained for the $x-z$ plane of bending of the shaft:

$$P_x = \frac{12EI}{a^3}\left(\frac{3a+L}{3a+4L}\right) X - \frac{6EI}{a^2}\left(\frac{3a+2L}{3a+4L}\right) \phi_y = K_{11}\, X + K_{12}\, \phi_y \tag{9}$$

$$M_y = -\frac{6EI}{a^2}\left(\frac{3a+2L}{3a+4L}\right) X + \frac{4EI}{a}\left(\frac{3a+3L}{3a+4L}\right) \phi_y = K_{21}\, X + K_{22}\, \phi_y \tag{10}$$

Similarly, using signs which agree with the system of co-ordinates, for the $y-z$ plane of bending of the shaft:

$$P_y = \frac{12EI}{a^3}\left(\frac{3a+L}{3a+4L}\right) Y + \frac{6EI}{a^2}\left(\frac{3a+2L}{3a+4L}\right) \phi_x = K_{11}\, Y - K_{12}\, \phi_x \tag{11}$$

$$M_x = \frac{6EI}{a^2}\left(\frac{3a+2L}{3a+4L}\right) Y + \frac{4EI}{a}\left(\frac{3a+3L}{3a+4L}\right) \phi_x = -K_{21}\, Y + K_{22}\, \phi_x \tag{12}$$

Disk Dynamical Forces and Moments

The internal reaction forces and moments acting on the disk will be replaced by the external forces and moments due to damping and disk unbalance and the dynamical or inertia forces and moments acting on the shaft.

From Newton's second Law of Motion

$$\sum \vec{\mathbf{F}}_{external} = m\, \vec{\mathbf{a}}$$

$$\text{or} \qquad \sum \vec{\mathbf{F}}_{external} + \vec{\mathbf{F}}_{inertia} = 0 \tag{13}$$

For the x direction the external forces F_x are

$$F_{x\ external} = m\, e_u\, \omega^2 \cos \omega t - C_d \dot{X}$$

Where C_d = disk damping ; e_u = mass unbalance eccentricity.

The inertia force in the x direction is

$$F_{x\ inertia} = -m\, \ddot{X}$$

Therefore the reaction load P_x is represented by

$$P_x = -m\, \ddot{X} - C_d\, \dot{X} + m\, e_u \omega^2 \cos \omega\, t \tag{14}$$

This expression includes a rotating unbalance at the end of the disk in which the disc mass center is displaced from the axis of rotation by e_u.

The reaction force P_y in the vertical direction is given by

$$P_y = -m\, \ddot{Y} - C_d\, \dot{Y} + m\, e_u\, \omega^2 \sin \omega\, t \tag{15}$$

For the rotational degrees of freedom, the equations of motion are given by

$$\vec{\mathbf{M}}_{external} + \vec{\mathbf{M}}_{inertia} = 0$$

$$\text{Where } \vec{\mathbf{M}}_{inertia} = -\frac{d\vec{\mathbf{H}}}{dt} \tag{16}$$

For small angular rotations of the disk, as shown in Fig. 3, the angular rotations of the disk, the angular momentum vector may be expressed as

$$\vec{\mathbf{H}} = I_p\, \omega\, \vec{k} + I_t\, \dot{\phi}_x\, \vec{i} + I_t \dot{\phi}_y\, \vec{j} \tag{17}$$

The total time rate of change of the angular momentum vector is given by

$$\frac{d\vec{\mathbf{H}}}{dt} = \left(\frac{\partial \mathbf{H}}{\partial \mathrm{t}}\right)_{local} + \vec{\omega}_{disk}\, X\, \vec{\mathbf{H}} \tag{18}$$

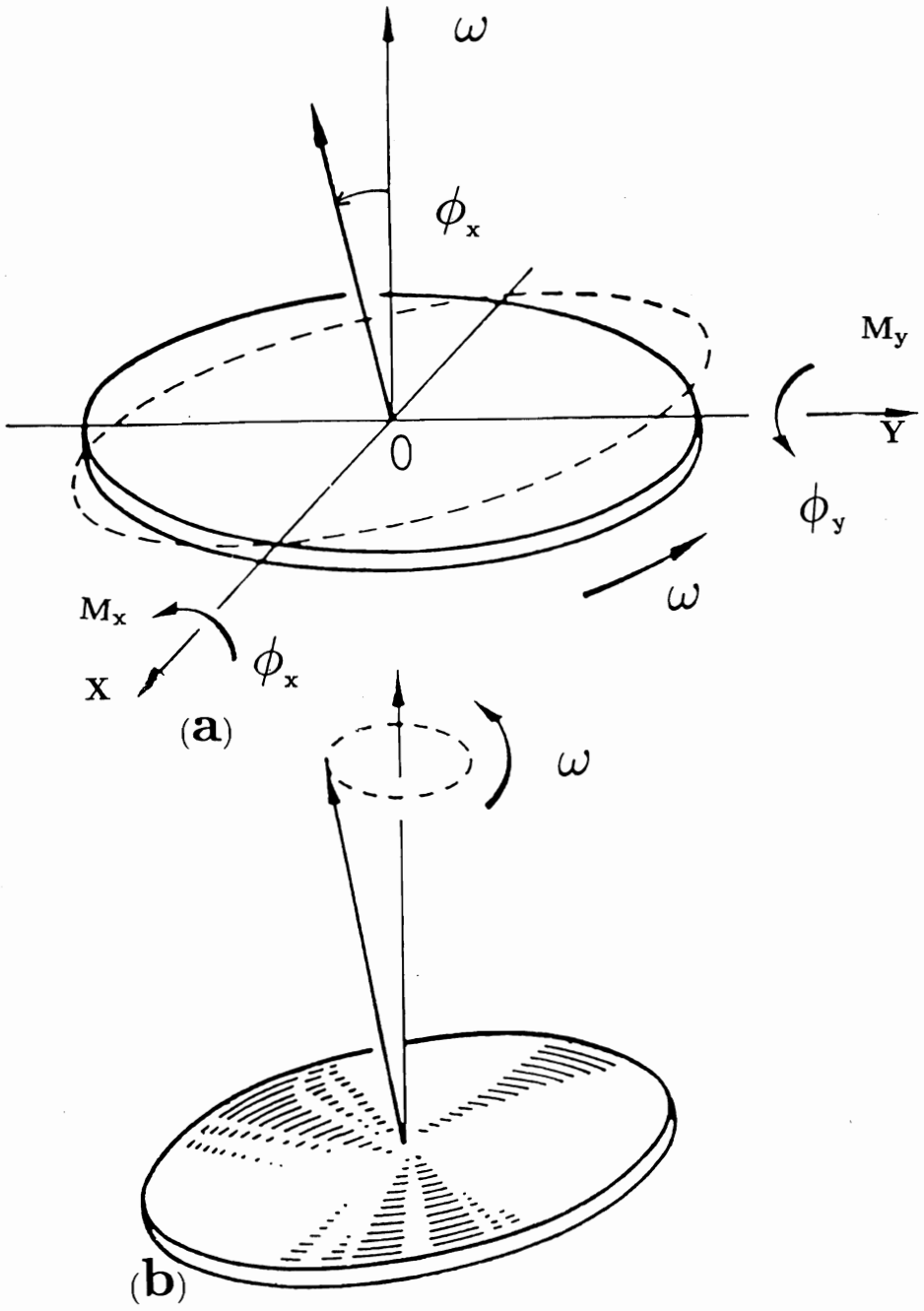

Fig. 3 Disk Angular Displacements and Moments for Small Rotations (Dimentberg).

$$\text{Where } \vec{\omega}_{\text{disk}} = \dot{\phi}_{\text{x}}\,\vec{\text{i}} + \dot{\phi}_{\text{y}}\,\vec{\text{j}}$$

$$\frac{d\vec{\mathbf{H}}}{dt} = I_p\,\dot{\omega}\vec{k} + I_t\,\ddot{\phi}_x\vec{i} + I_t\,\ddot{\phi}_y\,\vec{j}$$

$$+\left(\dot{\phi}_x\vec{i} + \dot{\phi}_y\vec{j}\right)\; X\left(I_t\,\dot{\phi}_x\vec{i} + I_t\,\ddot{\phi}_y\,\vec{j} + \omega\,I_p\,\vec{k}\right)$$

Assuming constant angular velocity ω we obtain for $\frac{d\vec{H}}{dt}$ the following:

$$\frac{d\vec{\mathbf{H}}}{dt} = \left(I_t\ddot{\phi}_x + \omega I_p\dot{\phi}_y\right)\vec{i} + \left(I_t\ddot{\phi}_y - \omega I_p\dot{\phi}_x\right)\vec{j} \tag{19}$$

Therefore the corresponding values of M_x and M_y are

$$M_{x\ inertia} = -\left(I_t\ddot{\phi}_x + \omega I_p\dot{\phi}_y\right) \tag{20}$$

$$M_{y\ inertia} = -\left(I_t\ddot{\phi}_y - \omega I_p\dot{\phi}_x\right) \tag{21}$$

An alternative derivative to the time rate of change of the angular momentum vector $\vec{\mathbf{H}}$ is to write the angular moment vector components along the fixed X and Y axes assuming small rotation angles. As illustrated by Dimentberg shown in Fig. 4, angular momentum components in the X and Y directions are given by

$$H_x = I_t\,\dot{\phi}_x + I_p\,\omega\,\phi_y \tag{22}$$

$$H_y = I_t\,\dot{\phi}_y - I_p\,\omega\,\phi_x \tag{23}$$

$$M_x = \frac{d\,H_x}{dt} = I_t\,\ddot{\phi}_x + I_p\,\omega\,\dot{\phi}_y \tag{24}$$

$$M_y = \frac{d\,H_y}{dt} = I_t\,\ddot{\phi}_y - I_p\,\omega\,\dot{\phi}_x \tag{25}$$

When small rotations are assumed the moment equations are linearized expressions in terms of the rotation angles as measured in a fixed coordinate system. The equations for the time rate of change of angular momentum as derived in Eqs. 24 and 25 are identical to those given in Eqs. 20 and 21.

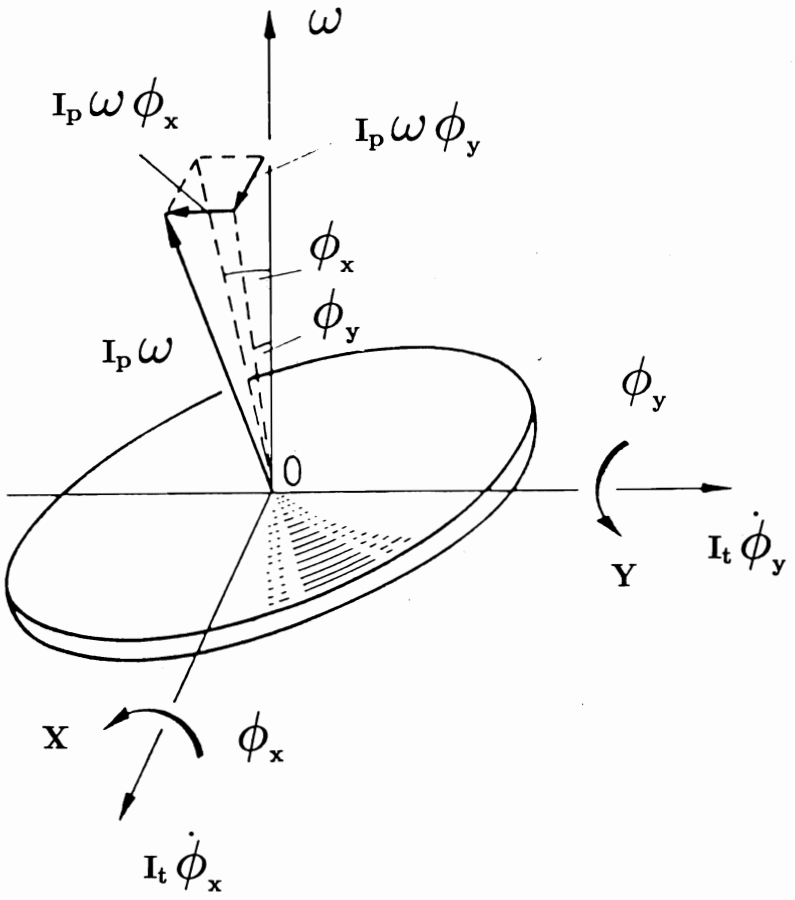

Fig. 4 Disk Angular Momentum Vector for Small Rotations (Dimentberg).

The disk kinetic eneregy as expressed in a fixed cooridnate system may be expressed as the sum of the kinetic energy of translation plus the kinetic energy of rotation, which includes the gyroscopic effect

$$T = T_{translations} + T_{rotations} \tag{26}$$

$$\begin{aligned} T &= \tfrac{1}{2} m \left(\dot{X}^2 + \dot{Y}^2\right) \\ &+ \tfrac{1}{2} I_t \left(\dot{\phi}_x^2 + \dot{\phi}_y^2\right) + \omega I_p \left(\phi_y \dot{\phi}_x - \phi_x \dot{\phi}_y\right) \end{aligned} \tag{27}$$

Disk Equations of Motion

Substituting the expressions P_x, P_y, M_y and M_x from Equations (14,15,20,21) in Equations (9-12), the differential equations for the free transverse vibrations of a rotating shaft at the end when friction forces are absent are obtained.

$$m\ddot{X} + C_d \dot{X} + K_{11} X + K_{12} \phi_y = m e_u \omega^2 \cos \omega t \tag{28}$$

$$m\ddot{Y} + C_d \dot{Y} + K_{11} Y - K_{12} \phi_x = m e_u \omega^2 \sin \omega t \tag{29}$$

$$I_t \ddot{\phi}_y - I_p \omega \dot{\phi}_x + K_{21} X + K_{22} \phi_y = 0 \tag{30}$$

$$I_t \ddot{\phi}_x + I_p \omega \dot{\phi}_y - K_{21} Y + K_{22} \phi_x = 0 \tag{31}$$

The four equations of motion may be combined into two complex equations of motions because of the symmetry of the shaft stiffness matrix.

$$\text{Let} \quad \mathbf{Z} = X + iY \;\; ; \;\; \phi = \phi_y - i\phi_x$$

The complex equations of motion including rotor radial unbalance e_u and disk skew τ are

$$m\ddot{\mathbf{Z}} + C_d \dot{\mathbf{Z}} + K_{11} \mathbf{Z} + K_{12} \phi = m e \omega^2 e^{i\omega t} \tag{32}$$

$$I_t \ddot{\phi} - i\omega I_p \dot{\phi} + K_{21} \mathbf{Z} + K_{22} \phi = \tau \omega^2 \left(I_p - I_t\right) e^{i(\omega t - \alpha)} \tag{33}$$

Undamped Forward and Backward Critical Speeds

In the absence of disk unbalance and external damping, it is assumed that the free undamped motion obeys harmonic motion of the form

$$z = Z\,e^{i\lambda t} \quad ; \quad \phi = \Phi\,e^{i\lambda t} \quad . \tag{34}$$

For the determination of the rotor undamped forward and backward critical speeds, the rotor damping and rotor unbalance are ignored. A harmonic motion of λ rad/sec is assumed. Positive values of λ relate to forward critical speeds. Negative values of λ correspond to backward critical speeds. For the case where $\lambda = \omega$, this is referred to as the synchronous critical speeds.

Substituting Eq.31 in Eqs.32 and 33, the characteristic is obtained from the equations of motion for free vibrations.

$$\begin{vmatrix} -m\lambda^2 + K_{11} & K_{12} \\ K_{21} & -I_t\lambda^2 + I_p\omega\lambda + K_{22} \end{vmatrix} = 0 \tag{35}$$

Expanding the determinant to form the characteristic equation

$$\lambda^4 - \frac{I_p}{I_t}\omega\lambda^3 - \left(\frac{K_{11}}{m} + \frac{K_{22}}{I_t}\right)\lambda^2 + \frac{I_p}{I_t}\,\frac{K_{11}}{m}\,\omega\lambda + \frac{K_{11}K_{22} - K_{12}^2}{I_t\,m} = 0.$$

For the case of a disc ($I_p = 2I_t$) the equation has the form:

$$\lambda^4 - 2\omega\lambda^3 - \left(\frac{K_{11}}{m} + \frac{K_{22}}{I_t}\right)\lambda^2 + 2\frac{K_{11}}{m}\omega\lambda + \frac{K_{11}K_{22} - K_{12}^2}{I_t\,m} = 0 \tag{36}$$

Equation 35 has two positive and two negative roots. The positive roots represent the forward critical speeds and the negative roots of λ represent the backward critical speeds. Dimentberg shows that the equivalent backward modes of λ may be obtained also by a sign change of ω. When ω is zero, there are two natural frequencies. These natural frequencies are referred to as the planar modes of motion. These would be the corresponding modes that would be obtained by a stationary rap test on the rotor.

The synchronous critical speeds are those values of ω which are simultaneously equal to the frequencies of the natural vibrations of the rotating shaft. Assuming that $\omega = \pm\lambda$, instead of Eq. 34 then follows

$$\omega^4 \pm \left(\frac{K_{22}}{I_t} \mp \frac{K_{11}}{m}\right)\omega^2 \pm \frac{K_{11}K_{22} - K_{12}^2}{I_t m} = 0 \tag{37}$$

Eq. 37 with the 'upper' signs has one real root (with plus or minus)

$$\omega_{if} = \sqrt{-\frac{1}{2}\left[\left(\frac{K_{22}}{I_t} - \frac{K_{11}}{m}\right) - \sqrt{\left(\frac{K_{22}}{I_t} + \frac{K_{11}}{m}\right)^2 - \frac{4K_{12}^2}{I_t m}}\right]} \tag{38}$$

This is the 1st forward synchronous critical speed

$$\omega_{1b} = \sqrt{\frac{1}{2}\left[\left(\frac{K_{11}}{m} + \frac{K_{22}}{3I_t}\right) - \sqrt{\left(\frac{K_{11}}{m} - \frac{K_{22}}{3I_t}\right)^2 - \frac{4K_{12}^2}{3I_t m}}\right]} \tag{39}$$

This is the rotor 1st backward critical speed.

$$\omega_{2b} = \sqrt{\frac{1}{2}\left[\left(\frac{K_{11}}{m} + \frac{K_{22}}{3I_t}\right) + \sqrt{\left(\frac{K_{11}}{m} - \frac{K_{22}}{3I_t}\right)^2 + \frac{4K_{12}^2}{3I_t m}}\right]} \tag{40}$$

This is the rotor 2nd backward critical speed.

When the signs of ω and λ are the same, forward precession takes place; when they are different, reverse precession takes place. Consequently, a rotating shaft with a thin disc has one critical speed of forward precession (38) and two critical speeds of reverse precession (39), (40). These values satisfy the inequality

$$\omega_{2b} > \omega_{if} > \omega_{1b} \tag{41}$$

Example Calculation of the Forward and Backward Critical Speeds of an Overhung Shaft-Rigid Bearings

The derivation of the forward and backward critical speeds as presented by Dimentberg assumes that the bearings are rigid and that the precessive motion is circular in either the forward or the backward direction.

As an example, consider a uniform shaft supported on two rigid bearings. The span between the bearings is 60 cm (23.622 in.) and the overhand distance is a = 30 cm (11.81 in.). The shaft diameter is d = 2 cm (.787 in.). The disk diameter is D = 50 cm (19.685 in.) and the thickness h = 1 cm.

The second area moment of inertia I of the shaft is

$$I = \frac{\pi\, d^4}{64} = \frac{\pi\, 0.787^4}{64} = 0.01882 \text{ in}^4$$

$$\text{E} = 30\text{E}6 \text{ lb/in}^2 \; ; \; \text{EI} = 564,637 \text{ lb/in}^2$$

The shaft stiffness coefficients are given by

$$K_{11} = \frac{12EI}{a^3}\left(\frac{3a+L}{3a+4L}\right) = 5 \cdot 45\frac{EI}{a^3} = 0 \cdot 333 \times 10^3 \text{ kg/cm} = 1,866 \text{ lb/in}$$

$$K_{12} = \frac{6EI}{a^2}\left(\frac{3a+2L}{3a+4L}\right) = -3 \cdot 82\frac{EI}{a^2} = -7 \cdot 0 \times 10^3 \text{ kg} = -15,477 \text{ lb}$$

$$K_{22} = \frac{4EI}{a}\left(\frac{3a+3L}{3a+4L}\right) = 3 \cdot 27\frac{EI}{a} = 179 \cdot 6 \times 10^3 \text{ kg} - \text{cm} = 155,560 \text{ lb} - \text{in}$$

The weight of the disk is

$$w = \frac{\pi\, D^4\, h}{4} \times 0.283 \text{ lb/in}^3 = 33.91 \text{ lb}$$

The polar moment of inertia is given by

$$I_p = m\frac{R^2}{2} = \frac{w}{g} \times \frac{R^2}{2} = \frac{1,643 \text{ lb} - \text{in}^2}{386 \text{ in/sec}^2} = 4.256 \text{ lb} - \text{sec}^2 - \text{in}$$

For a thin disk, the transverse moment of inertia is given by

$$I_t = \frac{m\,R^2}{4} = \frac{822 \text{ lb} - \text{in}^2}{386 \text{ in/sec}^2} = 2.13 \text{ lb} - \text{sec}^2 - \text{in}$$

The calculated forward and backward critical speeds are given by

$$\omega_{1f} = 70 \text{ rad/sec} = 669 \text{ RPM}$$
$$\omega_{1b} = 50 \text{ rad/sec} = 478 \text{ RPM}$$
$$\omega_{2b} = 208.5 \text{ rad/sec} = 1,991 \text{ RPM}$$

Figure 5 represents the computed forward and backward critical speeds as derived by Dimentberg. The intersection of the straight line $\lambda = \omega$ with the critical speed plots represents the forward and backward modes. Note that with a rigid disk and no shaft mass, the gyroscopic effect causes the second critical speed to increase at a rate that the synchronous line $\lambda = \omega$ does not intersect with the second forward critical plot. Thus for the ideal case of the overhung disk, as given in this example, there is only one synchronous forward critical speed that can be excited by rotor unbalance.

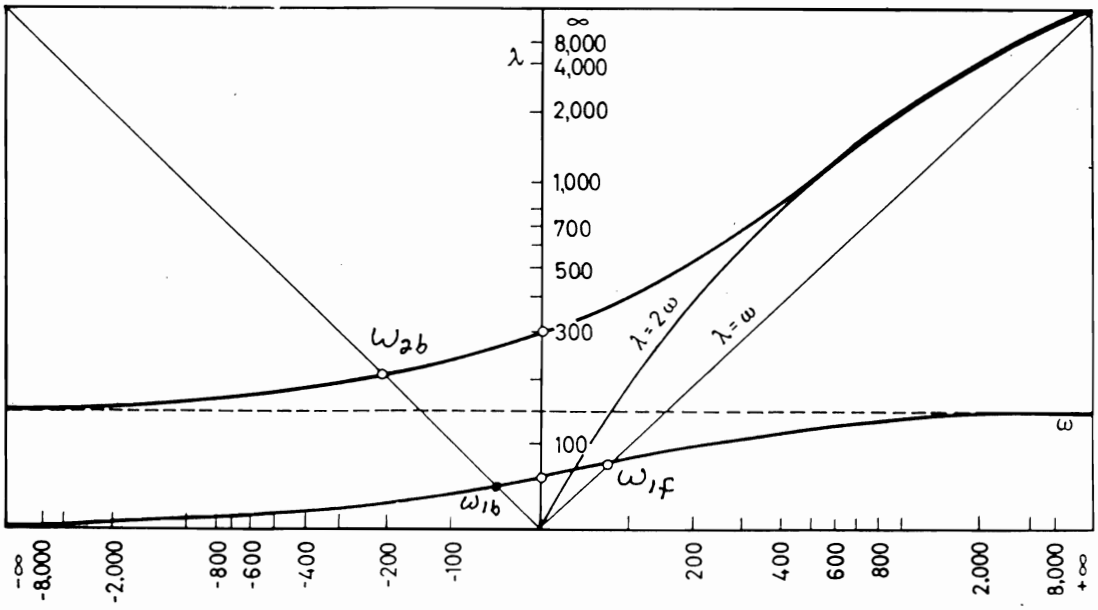

Fig. 5 Forward and Backward Critical Speeds of Overhung Rotor (Dimentberg)

A six-station model was generated using the CRITSPD-PC computer program to simulate the undamped forward and backward critical speeds of the overhung rotor. Critical speeds for the single-mass overhung rotor were computed with and without shaft mass included. For example, without the consideration of shaft mass, there is only one synchronous forward critical speed computed by the CRITSPD-PC program.

Table 1 represents the model for the single-mass overhung rotor. The disk was assumed attached to the shaft by a rotational spring stiffness of 1.0E8 lb-in. The external diameter of the disk is 19.685 in and the disk thickness is .3937 in. The specific weight of steel of .283 lb/in^3 was assumed. The value of the rotational spring rate K_{rot} of 1.0E8 lb-in treats the disk as if it were rigidly attached to the shaft.

In the first case, the bearing stiffnesses were assumed to be 1E7 lb/in. This value of stiffness essentially represents a rigid support. Figure 6 represents the overhung disk synchronous first critical speed including shaft mass. The first synchronous critical speed is computed to be 668 RPM. The theoretical predicted value of the first synchronous critical speed without shaft mass is shown to be 669 RPM. The inclusion of shaft mass causes only a very slight reduction of the first critical speed. The reason for this is that there is very little kinetic energy in the shaft as compared to the kinetic energy of the disk.

The inclusion of shaft mass, however, has a profound effect on the second critical speed. Without the inclusion of shaft mass in the model, there is no second critical speed predicted. However, when the shaft mass is included, there is a second critical speed predicted to be at 8,679 RPM as shown in Fig. 7. The kinetic energy of the system is predominantly in the shaft at the center span between the bearings. The overhung disk has become a nodal point where the deflection and slope approach zero. This behavior is typical of the motion observed on gas turbines with overhung fan sections. After the rotor speed exceeds the first critical speed, the fan section becomes a nodal point. Therefore balancing at the fan or the overhung disk location will have very little influence on the response at the second critical speed.

The forward and backward critical speeds for the overhung rotor were computed for a rotor speed of 2,000 RPM. The value of the first critical speed increases slightly in value as shown in the critical speed plot by Dimentberg in Fig. 5. For a rotor speed of 2,000 RPM, the second forward critical speed, neglecting shaft mass, as shown in Fig. 8 is 5,329 RPM. If the overhung rotor were in a gas turbine and were excited by the high rotor critical speed at 5,300 RPM, then the second forward critical speed could be excited.

Figure 9 represents the rotor backward first critical speed at 1,000 RPM. The mode shape is similar to the rotor first forward or synchronous critical speed. At 1,000 RPM, the backward mode occurs at 358 RPM. The backward precessive motion of the disk reduces the critical speed from the synchronous value of 669 RPM to 358 RPM. Figure 10 represents the overhung rotor second backward critical speed at 1,000 RPM. The mode shape is similar to the second forward critical speed except that there

TABLE 1 CRITICAL SPEED MODEL OF OVERHUNG ROTOR

```
                          --- CRITSPD-PC INPUT DATA SET ----

Number of Mass Stations          =  6
Number of Bearings               =  2
Number of Attached Discs         =  1
Number of Offset Flexible Discs  =  1

ROTOR IDENTIFICATION:
  OVERHUNG ROTOR MODEL BASED ON DIMENTBERG MODEL-BACKWARD MODES- 2,000 RPM
  RIGID DISK WITH NO SHAFT MASS - d = 2 CM , L=60 CM , A=30 CM
   DISK =50 CM X 1 CM ,  K BEARINGS =5E3

INITIAL ROTOR PARAMETERS:

Units In  (ENGLISH, MKS, or SI)          :   ENGLISH
Units Out (ENGLISH, MKS, or SI)          :   ENGLISH
Number of Modes to Calculate (0 to 10)   :   3
Calculate Shaft Gyroscopics (YES or NO)  :   NO
Calculate Shear Defomation (YES or NO)   :   NO
Global Value for Young's Modulus         :   30E6
Global Value for Shaft Density           :   0.00
Convergence Criterion                    :   1E-6
    F1=HELP; F2=SAVE FILE; F3=SAVE AND EXIT; F4=EXIT; ENTER=NEXT DATA FIELD

CRITSPD:  File = OVHDIMEN.DAT              Line =   21 Column =  1  INSERT OFF
Global Value for Young's Modulus         :   30E6
Global Value for Shaft Density           :   0.00
Convergence Criterion                    :   1E-6
Initial Shaft Z Coordinate               :   0.0

FLEXIBLE OFFSET DISC PARAMETERS:

    DISC  DISC    ROT      EXT     INT    POLAR    TRANS   DISC    DISC    DISC
    LOC  WEIGHT  STIFF     DIA     DIA    MOMENT   MOMENT  THICK   DENS   OFFSET
 1   6     0     1.0E8   19.685   0.0     0.00     0.00    .3937   0.283   0.0

ATTACHED DISC PARAMETERS:

       DISC       DISC       DISC       DISC     DISC  0=Left Justified
     LOCATION   DIAMETER   THICKNESS   DENSITY   TYPE  1=Centered
  1:   6          19.685     .3937      0.00001   1

ROTOR STATION PARAMETERS:

       EXT      STATION     EXT       INT      POLAR     TRANS      SHAFT     E
     WEIGHT     LENGTH      DIA       DIA      MOMENT    MOMENT     DENS     MOD
  1 :  0          .5        .787      0        0         0          0        1
  2 :  0         11.81      .787      0        0         0          0        1
    F1=HELP; F2=SAVE FILE; F3=SAVE AND EXIT; F4=EXIT; ENTER=NEXT DATA FIELD

CRITSPD:  File = OVHDIMEN.DAT              Line =   41 Column =  1  INSERT OFF
      WEIGHT    LENGTH      DIA       DIA      MOMENT    MOMENT     DENS     MOD
  1 :  0          .5        .787      0        0         0          0        1
  2 :  0         11.81      .787      0        0         0          0        1
  3 :  0         11.81      .787      0        0         0          0        1
  4 :  0          5.905     .787      0        0         0          0        1
  5 :  0          5.905     .787      0        0         0          0        1
  6 :  0          .2        .787      0        0         0          0        1

BEARING PARAMETERS:

     BEARING     BEARING     SUPPORT     SUPPORT
     LOCATION    STIFFNESS   STIFFNESS   WEIGHT
  1 :  2          5E3         0           0
```

is considerably more amplitude at the overhung disk location. If the foundation is excited at 2,300 RPM, then the 2nd backward whirl mode may be excited in the absence of damping on the rotor. The excitation of the foundation in a planar mode is similar to exciting the foundation by a simultaneous forward and backward rotating vector. The backward rotating vector would excite the backward mode. Normally with symmetric bearing stiffness characteristics, rotating unbalance will not excite the backward rotor mode.

As an additional check of the critical speeds of the overhung rotor, the finite element program DYROBES was used. The DYROBES finite element program has the ability to compute the complex or damped eigenvalues of the system. By specifying the rotor speed, the DYROBES program automatically computes the system forward and backward complex eigenvalues and mode shapes. In the DYROBES program, a bearing damping value of 0.1 lb-sec/in was used. Table 2 represents various forward and backward critical speeds computed using the theoretical single-mass overhung rotor equations, the CRITSPD program and the DYROBES program. Excellent agreement between the CRITSPD and DYROBES programs was obtained for the computed forward and backward modes of the overhung disk with and without shaft mass.

TABLE 2 COMPARISON BETWEEN THEORETICAL OVERHUNG DISK CRITICAL SPEEDS AND COMPUTER PREDICTIONS

Case	RPM	Shaft Mass	Forward Modes RPM		Backward Modes RPM		Bearing Stiffness lb/in		COMMENTS
			1_f	2_f	1_b	2_b	K_x	K_y	
1	Variable	No	676.7	—	—	—	10^8	10^8	Forward Synchronous **CRITSPD**
2	Variable	Yes	668	8,679	—	—	10^8	10^8	Forward Synchronous **CRITSPD**
3	Variable	No	670	—	479	1,983	Rigid	Rigid	Dimentberg Syn. For. & Back
4	2,000	No	907	5,329	247.6	1,994	10^8	10^8	**CRITSPD** For. & Back
5	2,000	No	907	5,324	247.8	1,994	10^7	10^7	**DYROBES** Complex Roots
6	2,000	No	—	—	240.7	1,612	5E3	5E3	Soft BRGs **CRITSPD** Backward Modes
7	2,000	No	795	5,049	240.9	1,614	5E3	5E3	Soft BRGs **DYROBES** Complex Roots
8	2,000	Yes	785	4,951 6,517	240.4	1,591	5E3	5E3	Soft BRGS **DYROBES** Shaft Mass
9	2,000	No	818	5106	242	1,693	5E3	10E3	**DYROBES** BRG Asymmetry

CRITSPD-PC - Undamped critical speed analysis program by transfer matrix method
DYROBES - Finite element rotor program with QR method for complex roots

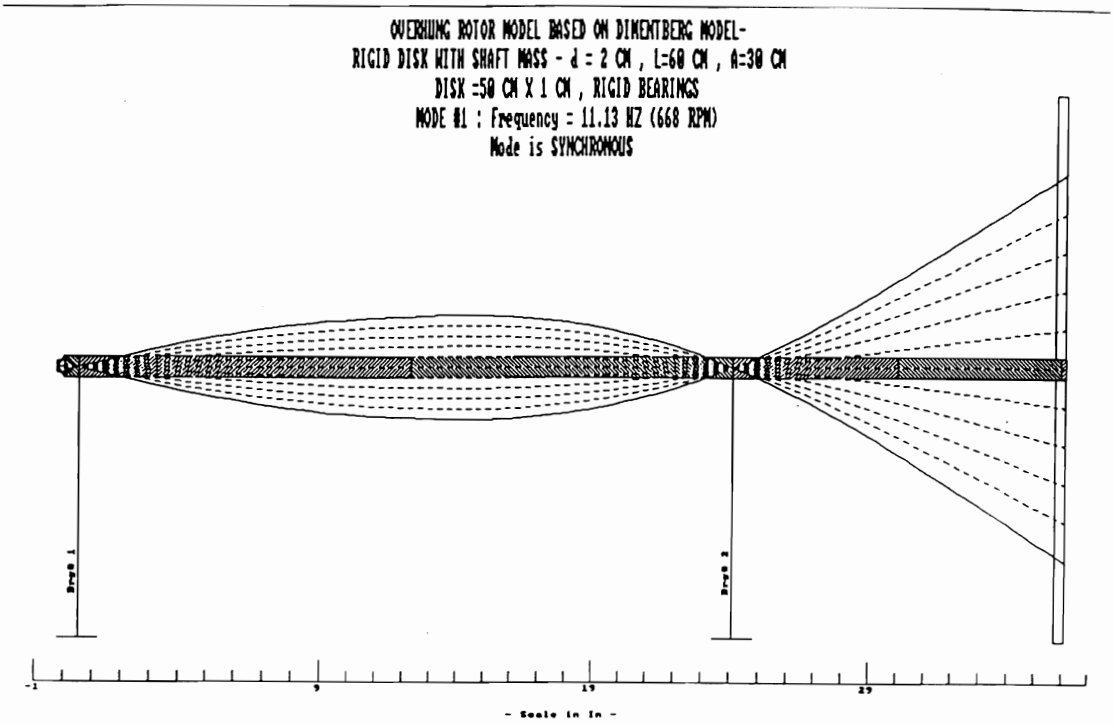

Fig. 6 Overhung Disk Synchronous 1st Critical Speed Including Shaft Mass ; $N_1 = 688$ RPM

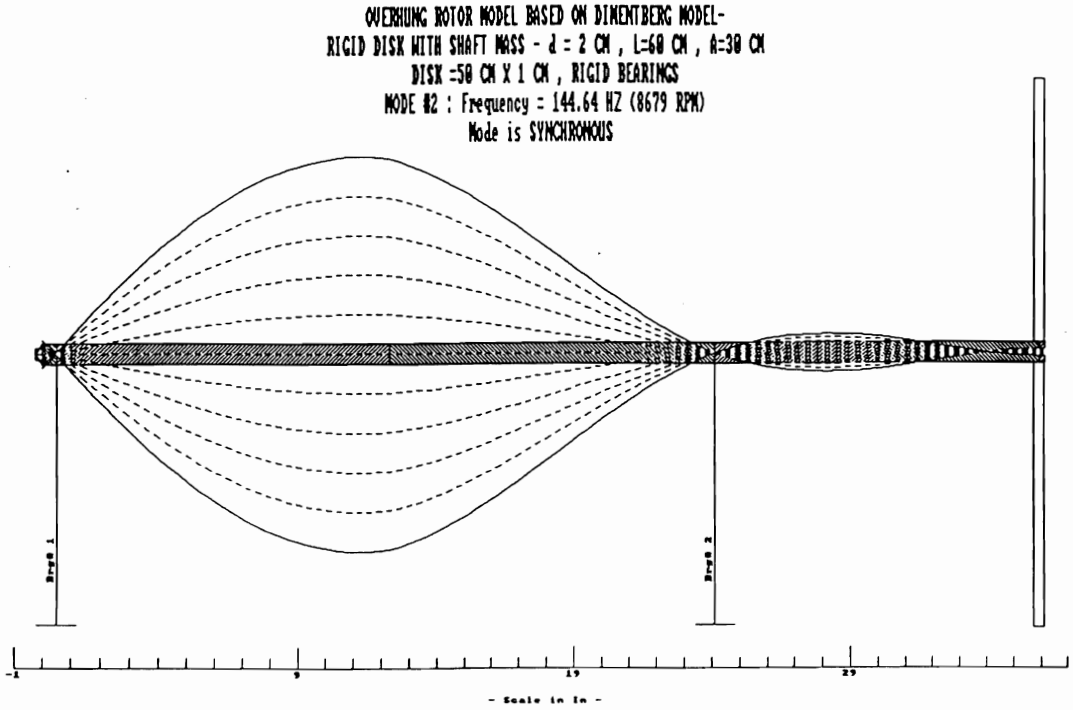

Fig. 7 Overhung Rotor Second Critical Speed Including Shaft Mass $N_2 = 8{,}079$ RPM

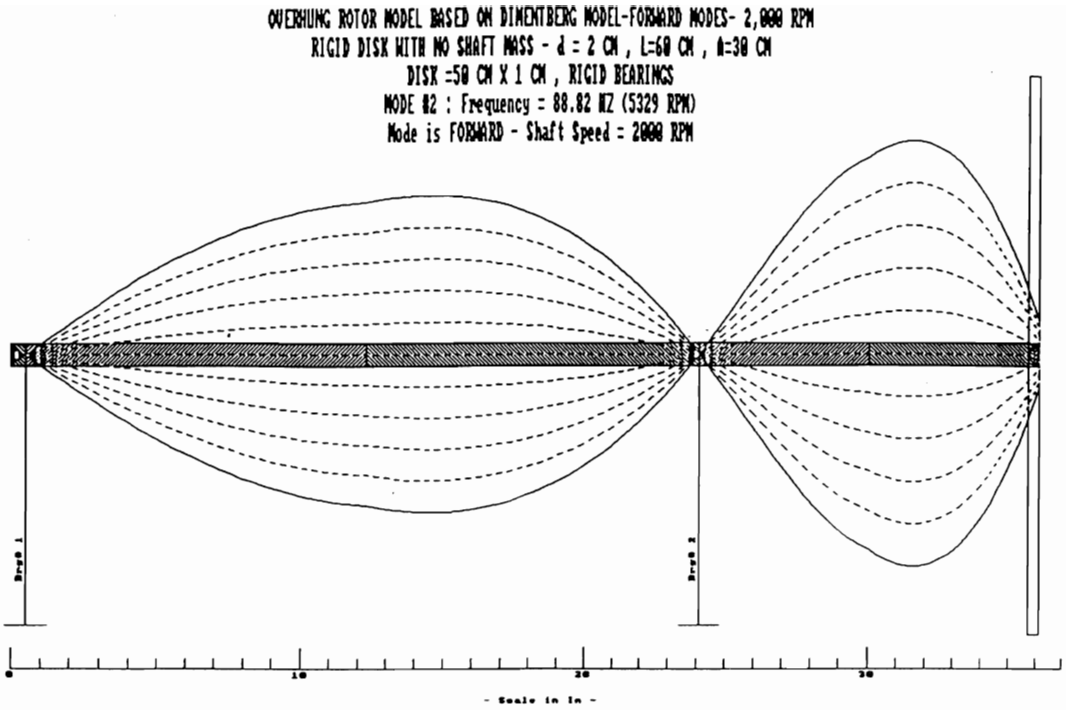

Fig. 8 Overhung Disk 2nd Forward Critical Speed With No Shaft Mass at N=2,000 RPM ; N_{2f}=5,329 RPM

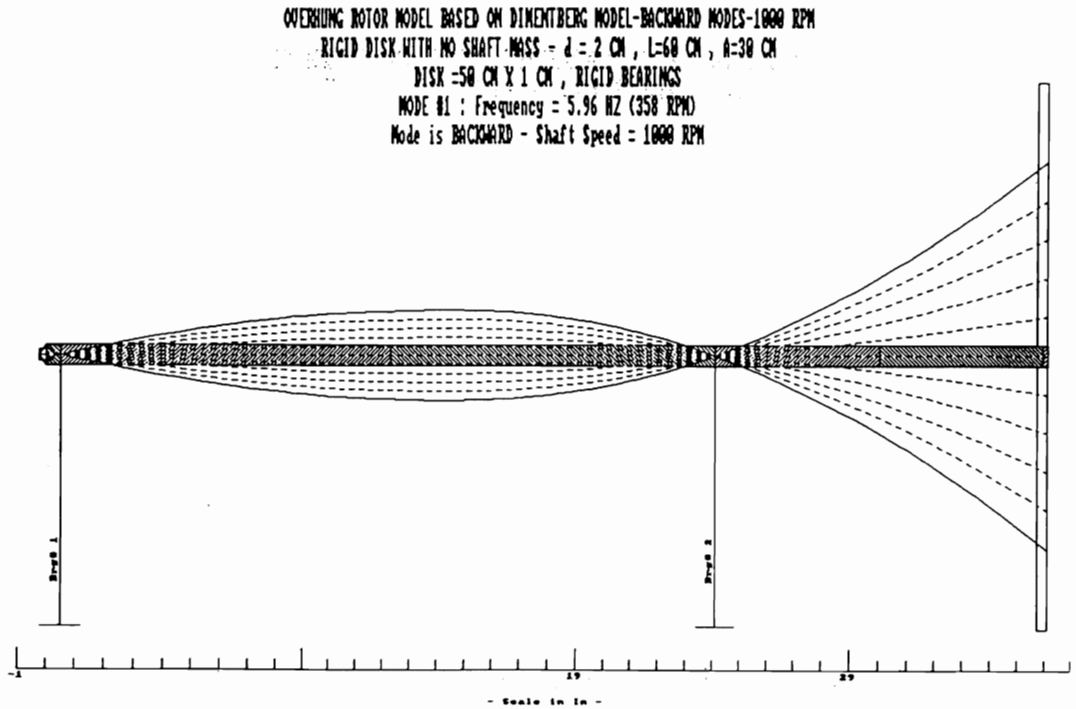

Fig. 9 Overhung Rotor Backward 1st Critical Speed at 1,000 RPM N_{b1}=350 RPM

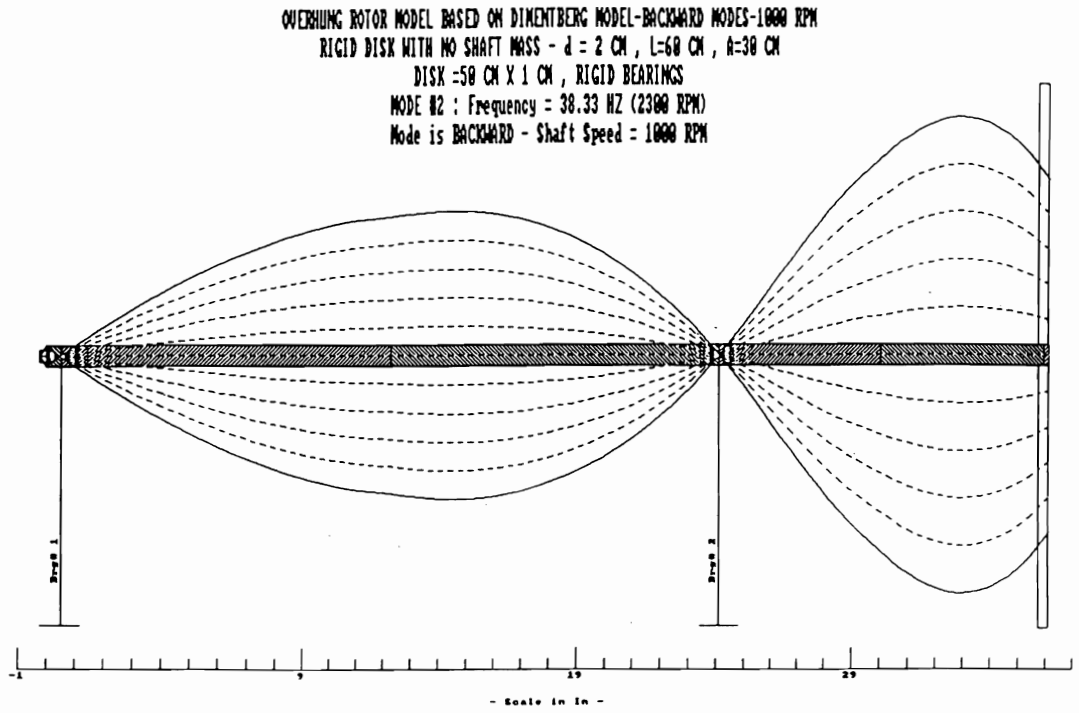

Fig. 10 Overhung Rotor 2nd Backward Critical Speed at 1,000 RPM N_{b2}=2,300 RPM

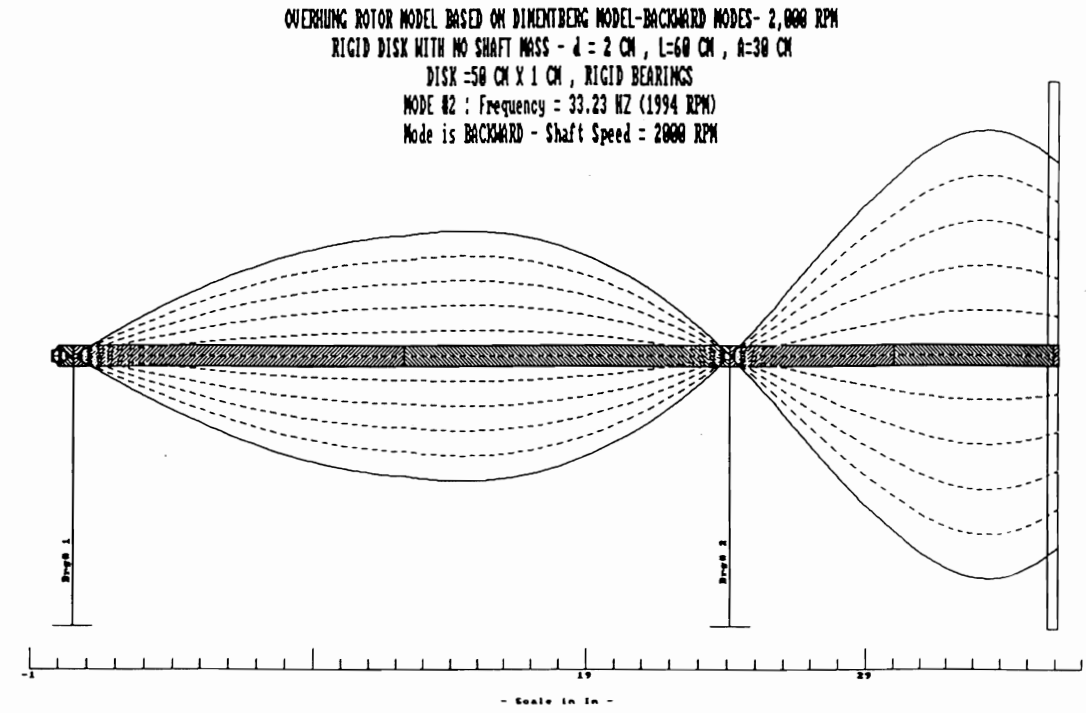

Fig. 11 Overhung Disk 2nd Backward Mode at 2,000 RPM N_{b2}=1,994 RPM

Forced Response of the Overhung Rotor with Bearing Asymmetry.

Figure 12 represents a schematic of the overhung rotor that was used in the DYROBES program. In the DYROBES program, the horizontal and vertical values of the bearing stiffness may be changed. In the critical speed program, for example, only one value of bearing stiffness may be assumed. The rotor orbits are either forward or backward circular orbits. The use of bearing asymmetry results in elliptical orbits, which can change the gyroscopic effects of the disk on the shaft.

Figure 13, for example, represents the synchronous unbalance response at the overhung location with unbalance at the disk location. The peak response occurs at 550 RPM assuming asymmetric bearings of 2E3 lb/in. Notice that the phase change in the x and y direction is from 0 to 180 degrees, which is one would expect for the single-mass rotor. There is no indication at all of the existence of a second critical speed in this plot. Figures 14 and 15 represent the forces transmitted to the inboard and outboard bearings, respectively. The maximum force at the inboard bearing is approximately 6 lb at 550 RPM, and the maximum force at the outboard bearing is 20.5 lb at 550 RPM. The outboard bearing near the disk always has the highest forces transmitted at the first critical speed. Likewise, from the plot on bearing forces transmitted, there is no indication of the excitation of a higher mode.

In the next forced unbalance response run, as shown in Fig. 16, the vertical bearing stiffness is 1E4 lb/in and the horizontal bearing stiffness is 5E3 lb/in. This represents a difference in bearing stiffness in the x and y directions by a factor of 2 with stiffer bearings than in Fig. 15. A peak critical speed is shown at 620 RPM. It is also of interest to note that the first backward and second backward modes show an excitation by the unbalance on the disk. Figure 17 represents the outboard bearing forces transmitted. The outboard bearing forces transmitted have been increased to 100 lb at 620 RPM. The increase in bearing forces at the outboard bearing at the first critical speed is due to the use of stiffer bearings. However, because of bearing asymmetry, one can also see the excitation of the second backward critical speed at approximately 1750 RPM.

In the next unbalance response case as shown in Fig. 18, the bearing stiffness in the y direction is 2E3 lb/in, which corresponds to the first case. The horizontal bearing stiffness has been reduced by a factor of 4 to 5E2 lb/in. There are two distinct first criticals in the x and y directions due to the asymmetric support system. Of particular interest is the strong appearance of the second backward critical speed at 1,260 RPM which is now excited by unbalance. This figure should be compared to Fig. 13. which represents the rotor response on symmetric bearing supports. By reducing the stiffness in the horizontal direction by a factor of 4, a strong excitation of the second backward critical speed is seen at 1,260 RPM. Figure 19 represents the bearing forces transmitted at the outboard bearing. The maximum bearing force is 56.5 lb at 1,260 RPM, which corresponds to the second backward critical speed. Figure 19 should be compared to the forces transmitted for Fig. 15, which shows only a 20.5 lb maximum transmitted at 550 RPM. Thus the incorporation of bearing

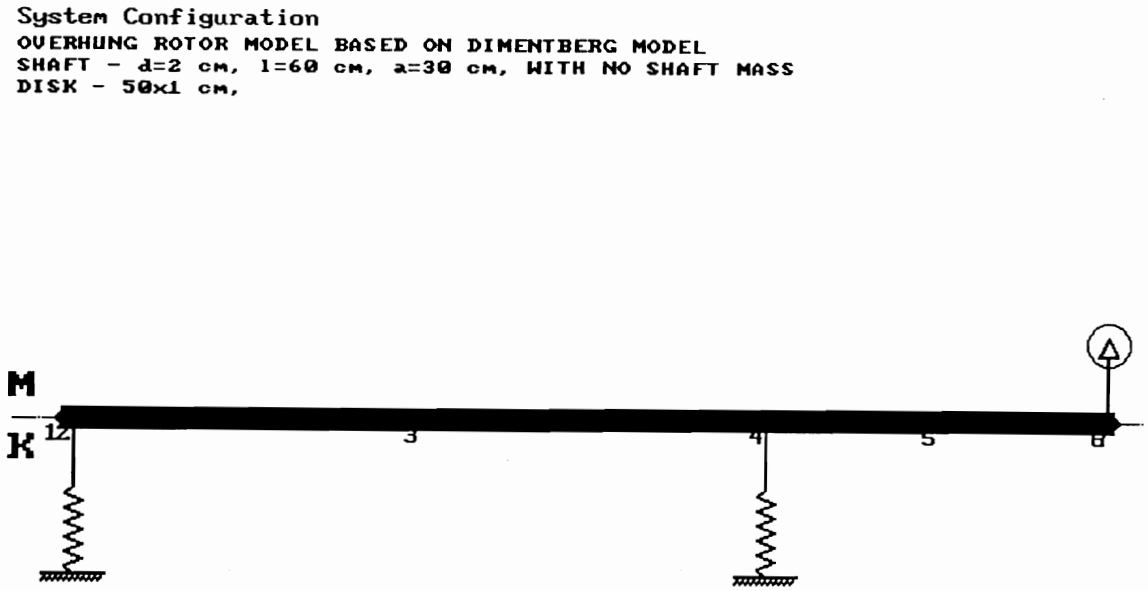

Fig. 12 Finite Element Model of Overhung Rotor Using DYROBES

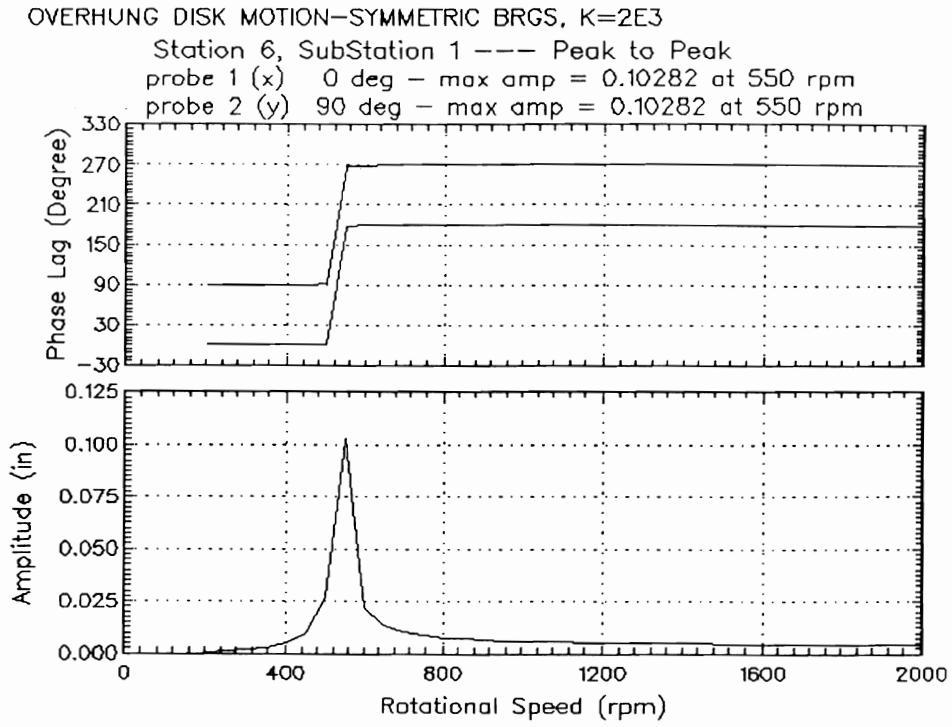

Fig. 13 Synchronous Unbalance Response of the Overhung Disk With Symmetric Bearing Stiffness Characteristics

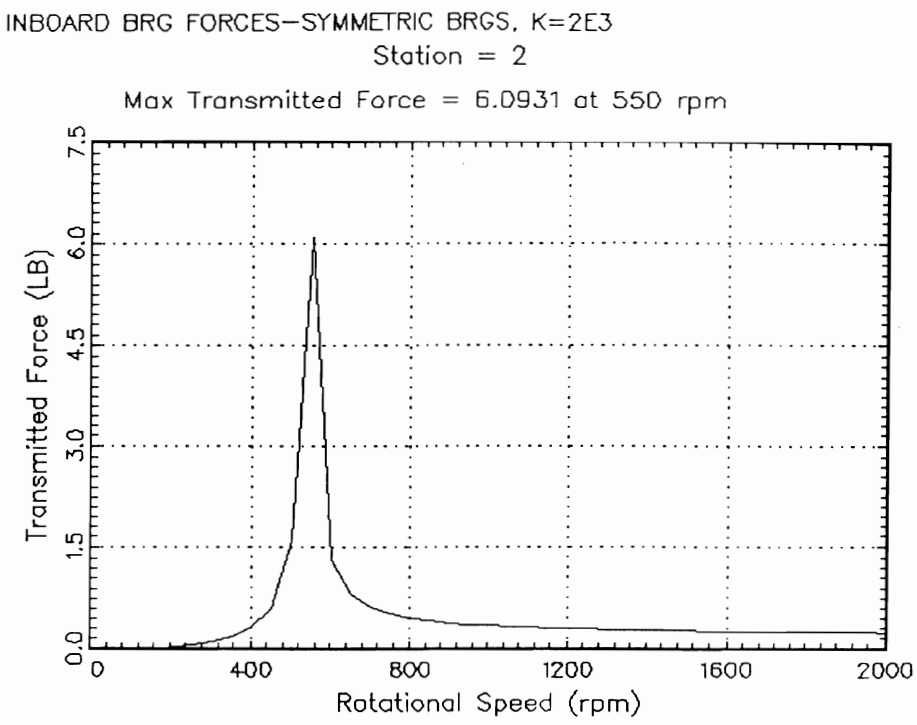

Fig. 14 Inboard Bearing Forces Transmitted With Symmetric Bearings K=2E3 lb/in

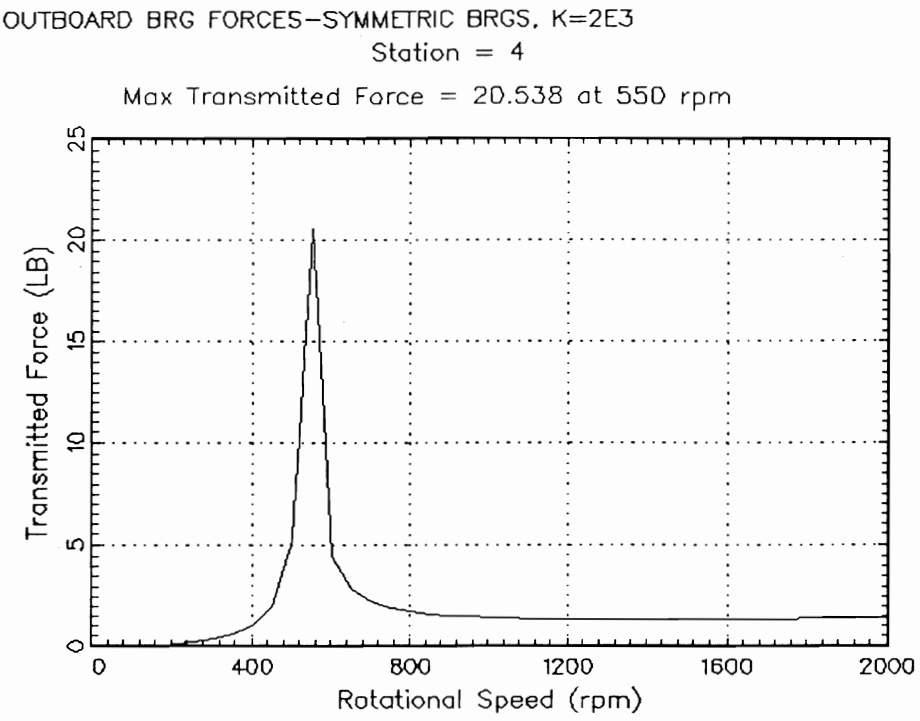

Fig. 15 Outboard Bearing Forces Transmitted With Symmetric Bearings ; K=2E3 lb/in

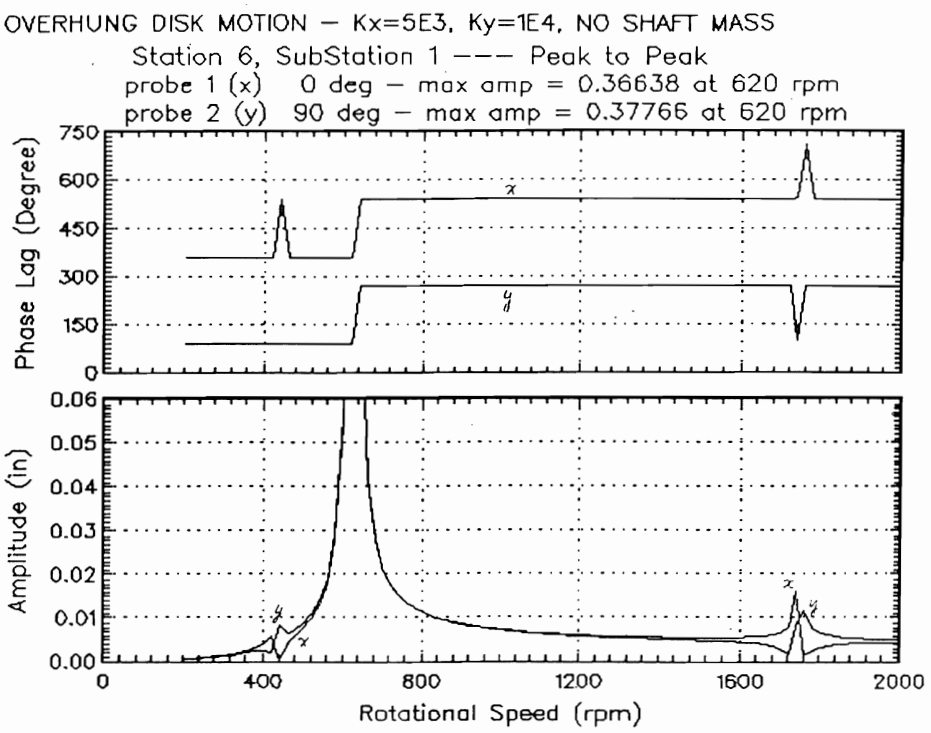

Fig. 16 Unbalance Response of Overhung Disk With Bearing Asymmetry ; K_x = 5E3 lb/in , K_y = 1E4 lb/in

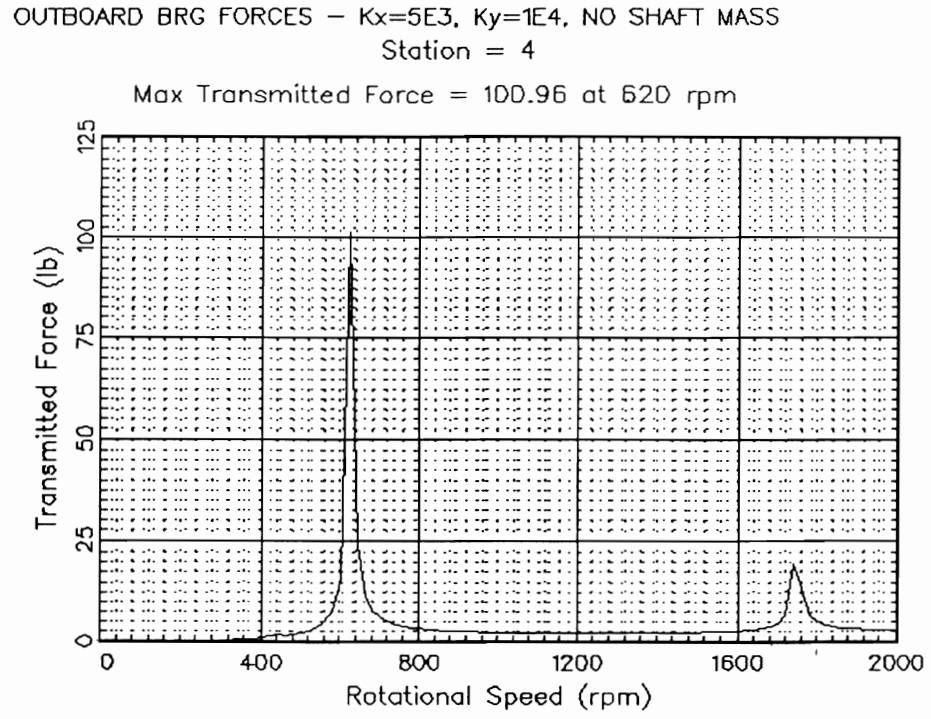

Fig. 17 Outboard Bearing Forces Transmitted With Bearing Asymmetry ; K_x = 5E3 lb/in , K_y = 1E4 lb/in

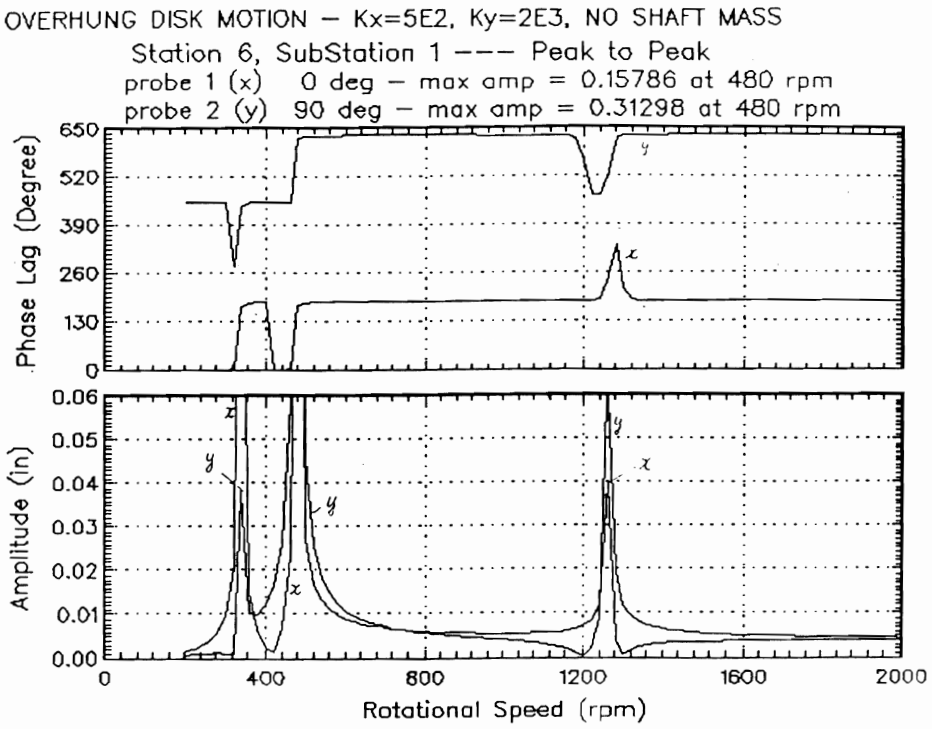

Fig. 18 Unbalance Response of Overhung Disk With Bearing Asymmetry ; K_y = 2E3 lb/in , K_x = 5E2 lb/in

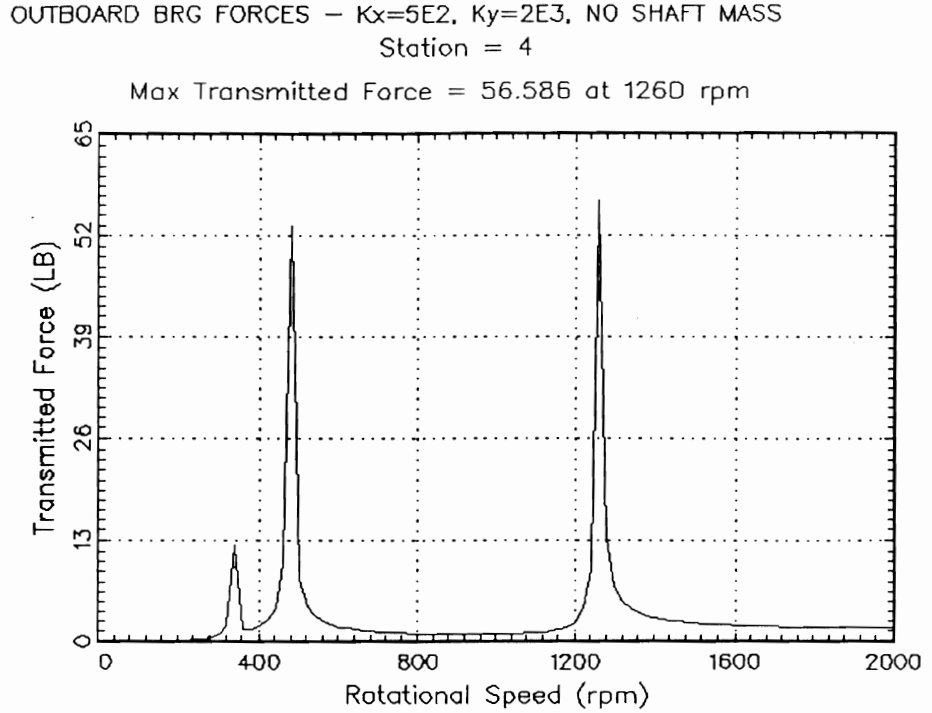

Fig. 19 Outboard Bearing Forces Transmitted With Bearing Asymmetry ; K_y = 2E3 lb/in , K_y = 5E2 lb/in

asymmetry has caused a substantial excitation of the second backward critical speed due to unbalance. If bearing symmetry is maintained, then the high response at 1260 RPM is not seen.

Therefore we see that in the case of an overhung rotor with bearing asymmetry, there is a strong possibility that a second backward whirl may be excited. Although this effect was eluded to by Dimentberg, at the time he studied this, computer programs such as the **DYROBES** finite element program were not in existence in order to calculate such an effect. It is possible that overhung aircraft gas turbines with uncentered squeeze film dampers may exhibit the asymmetric effect due to gravitational loading and aircraft manuevers. This may then lead to the excitation of the turbine backward second critical speed.

References

Dimentberg, F.M., "*Flexural Vibrations of Rotating Shafts*," Butterworth, London, 1961.

Gunter, E.J. and C.G. Gaston, "*CRISTPD-PC User's Manual*," RODYN Vibration, Charlottesville, VA, 1987.

Chen, W.J., "*DYROBES—Dynamics of Rotor Bearing System User's Manual*," Ver. 2.0, Dynamic Elegance, Chandler, AZ 85226, March 1992.